nature climate change

ARTICLES

https://doi.org/10.1038/s41558-020-0746-8

Agricultural risks from changing snowmelt

Yue Qin[1,2,3]✉, John T. Abatzoglou[4,5], Stefan Siebert[6], Laurie S. Huning[7], Amir AghaKouchak[3,7], Justin S. Mankin[8,9,10], Chaopeng Hong[3], Dan Tong[3], Steven J. Davis[3,7] and Nathaniel D. Mueller[11,12]✉

Snowpack stores cold-season precipitation to meet warm-season water demand. Climate change threatens to disturb this balance by altering the fraction of precipitation falling as snow and the timing of snowmelt, which may have profound effects on food production in basins where irrigated agriculture relies heavily on snowmelt runoff. Here, we analyse global patterns of snowmelt and agricultural water uses to identify regions and crops that are most dependent on snowmelt water resources. We find hotspots primarily in high-mountain Asia (the Tibetan Plateau), Central Asia, western Russia, western US and the southern Andes. Using projections of sub-annual runoff under warming scenarios, we identify the basins most at risk from changing snowmelt patterns, where up to 40% of irrigation demand must be met by new alternative water supplies under a 4 °C warming scenario. Our results highlight basins and crops where adaptation of water management and agricultural systems may be especially critical in a changing climate.

Irrigation is the largest use of water worldwide, accounting for more than 85% of global consumption[1,2]. In return, irrigated croplands produce roughly 30–40% of the world's food calories, although only about 20–25% of harvested crop areas are irrigated[3,4]. Climate change may alter the availability of water for irrigation, threatening the productivity of irrigated crops and projected growth in irrigated areas (for example, ~16% increases from 2000 to 2030)[5].

The majority of irrigation water worldwide is supplied by surface water[6] and patterns of surface water availability are expected to change substantially in a warming climate[7]. Although many studies have evaluated the agricultural risks from projected changes in annual precipitation and drought[8,9], relatively few have focused on the implications of sub-annual changes in surface runoff[10]. Water demands vary considerably across seasons due to crop phenology[11]; even if the magnitude of annual runoff is unchanged in the future, shifts in the timing of runoff may have profound implications for irrigated crops.

Seasonal distributions of runoff are highly sensitive to changes in snowpack accumulation and melt. In basins where a large share of precipitation falls in the winter as snow, the resulting runoff can be delayed until the snow melts in spring and summer[12–14]. The importance of snow as a seasonal water resource is well-acknowledged[15,16], but existing analyses are limited. Most previous studies emphasize the importance of snow to water availability based on indirect annualized supply side measures, such as ratios of annual snowfall to precipitation[17] or to runoff[18]. A few studies have used process-based hydrological models to obtain more direct estimates of snowmelt contributions to total runoff for specific regions (considering important processes of sublimation and infiltration)[14,19]. However, these studies rarely take unique patterns of agricultural water demand into account[14,18,19]. Those few studies that consider both snowmelt water supply and demand only provide an aggregated annual or season-total picture[20], and often infer snowmelt contributions to runoff rather than explicitly simulating it[21], introducing key physical uncertainties. So far no global studies have effectively analysed sub-annual snowpack and runoff dynamics reconciled with the unique timing and magnitude of agriculture water demand to characterize the risks to irrigated agriculture from changing snowmelt, despite agricultural dependence on snowmelt having been considered a key climate change risk for many years[15,16].

Here we analyse the global dependence of irrigated agriculture on snowmelt runoff and characterize basin- and crop- specific risks from climate change (details of our analytical approach and methodological validations are provided in the Methods). In summary, we use the TerraClimate dataset[22] to quantify both the historical (1985–2015) magnitude of monthly runoff in each major basin (a modified version[21] of the Simulated Topological Network 30p; ref. [23]) and the fractions of runoff that are derived from rainfall and snowmelt. Using crop-specific estimates of monthly irrigation water demand based on the Global Crop Water Model[24], annual time series of area equipped for irrigation[25], and irrigation water source data (surface water versus groundwater)[6] for the same period, we then estimate the average fraction of surface water consumed by irrigation that is derived from snowmelt runoff (the share of irrigation demand met by snowmelt) in each corresponding basin. Unless otherwise stated, we only focus on surface water supply and demand and ignore all other sources. Our monthly accounting assumes rainfall and snowmelt runoff are used in proportion to their availability in each month. When surface water supplies in a given month are insufficient to meet the demands of irrigation and other sectors[26], we quantify the shortfall in surface water demand that may be met by alternative surface water sources such as stored runoff in reservoirs from previous months, inter-basin transfers and desalination. Finally, we repeat our analyses using changes in snowmelt and

[1]Department of Geography, The Ohio State University, Columbus, OH, USA. [2]Sustainability Institute, The Ohio State University, Columbus, OH, USA. [3]Department of Earth System Science, University of California, Irvine, Irvine, CA, USA. [4]Management of Complex Systems Department, University of California, Merced, Merced, CA, USA. [5]Department of Geography, University of Idaho, Moscow, ID, USA. [6]Department of Crop Sciences, University of Göttingen, Göttingen, Germany. [7]Department of Civil and Environmental Engineering, University of California, Irvine, Irvine, CA, USA. [8]Department of Geography, Dartmouth College, Hanover, NH, USA. [9]Department of Earth Sciences, Dartmouth College, Hanover, NH, USA. [10]Lamont–Doherty Earth Observatory of Columbia University, Palisades, New York, NY, USA. [11]Department of Ecosystem Science and Sustainability, Colorado State University, Fort Collins, CO, USA. [12]Department of Soil and Crop Sciences, Colorado State University, Fort Collins, CO, USA. ✉e-mail: qin.548@osu.edu; nathan.mueller@colostate.edu

rainfall runoff projected under both 2 °C and 4 °C warming scenarios as calculated by the TerraClimate dataset forced with multi-model changes in climate conditions (see Methods).

Figure 1 shows the share of average runoff from recent snowmelt (1985–2015; Fig. 1a) and the changes under mean warming of 2 °C and 4 °C (Fig. 1b,c, respectively). Snowmelt contributes ≥50% of runoff across 26% of the global land area, especially in western US, western China, Central Asia, the southern Andes and in high northern latitudes (Fig. 1a). By aggregating the gridded runoff to major river basins (Supplementary Fig. 1), we find that, as of 2015, ~600 million people (~8% of global population) lived in basins where on average over half of the annual runoff is snowmelt[27]. In addition, roughly 40% of the world's irrigated rye and barley production—and 20% of irrigated sugar beets, grapes, sunflower, potatoes and cotton production—are located in these snowmelt-dominated basins (although the overall surface water use for some of these crops is small; for example, ~0.8 km^3 for rye compared with ~46 km^3 for cotton).

Global warming induces substantial and progressive decreases in the fraction of runoff originating from snowmelt (Fig. 1b,c, red and orange shading), especially across the Tibetan plateau, Western Europe, southern Central Asia, western Iranian plateau, Turkey, the northeast and western US and the southern Andes. Such decreases are influenced in most regions by declines in the magnitude of snowmelt runoff and increases in rainfall runoff (Supplementary Fig. 2). Although climate change also increases snowmelt runoff (blue shading) in some parts of Russia, Canada and Alaska due to overall increases in precipitation (Supplementary Fig. 2a,b), the area where snowmelt averages ≥50% of annual runoff decreases from ~39 million km^2 (~26% of global land area) to ~37 million km^2 (~25%) under the 2 °C warming scenario and further decreases to ~33 million km^2 (~22%) under the 4 °C warming scenario. Likewise, the population living in these snowmelt-dominant regions (2015) falls from ~8% of global population to ~6% and ~3% in the 2 °C and 4 °C warming scenarios, respectively.

Figure 2 illustrates the relationship between monthly runoff (red and blue curves show rainfall and snowmelt, respectively; as derived from Supplementary Fig. 3) and monthly water demand (stacked bars) for all uses in selected basins where snowmelt currently meets a relatively large share of annual irrigation water demands. Taking the San Joaquin basin in California as an example (Fig. 2a), rainfall runoff is currently greatest during the winter months (solid red curve) when demand for water is at its lowest (bars); as demands increase in spring, almost all consumed runoff is snowmelt (solid blue curve, blue bars in May and June); total runoff almost disappears in summer, and alternative sources of water (for example, storage and inter-basin transfers) are necessary to meet surface water demand (dark grey bars).

Under both 2 °C and 4 °C warming scenarios, snowmelt runoff decreases in magnitude and shifts towards earlier spring (Fig. 2, dashed blue curves). Under the same scenarios, however, the magnitude of rainfall runoff increases but changes little with respect to timing (dashed red curves). Depending on both the magnitude and the timing, rainfall runoff increases may (for example, Indus) or may not (for example, San Joaquin) be able to compensate for the declines in snowmelt runoff in meeting irrigation water demand (Fig. 2 and Supplementary Fig. 4).

For each basin, we calculate the share of consumed irrigation water that is derived from snowmelt, rainfall and alternative sources, respectively (Methods; Extended Data Fig. 1). In most basins, the share of irrigation demand met by snowmelt (Extended Data Fig. 1) is much lower than the share of runoff from snowmelt (Fig. 1 and Supplementary Fig. 1), as the former reflects the temporal coincidence of irrigation demands and snowmelt runoff. Although surface water irrigation demands worldwide are mostly met by rainfall runoff, relatively large shares of irrigation demand

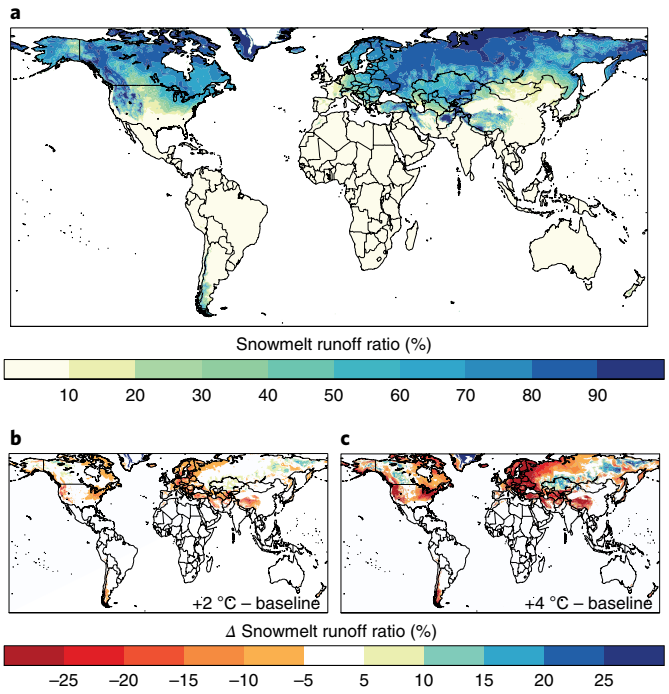

Fig. 1 | Geographical pattern of snowmelt runoff during recent decades (1985–2015) and under future warming scenarios. a–c, Based on historical data, the average ratio of annual runoff from snowmelt (**a**) is >80% in many areas, especially in the higher latitudes of the Northern Hemisphere. Under warming of 2 °C (**b**) and 4 °C (**c**), the share of runoff originating from snowmelt declines substantially in many of the same areas. Figures are displayed at a spatial resolution of 0.25 × 0.25°. Coastlines are from NCL/NCAR: http://www.ncl.ucar.edu/citation.shtml (see ref. [53]).

are met by snowmelt in parts of western China, Siberia, Argentina, Alaska and western Canada. Alternative sources of surface water are important in southern and central India, Central Asia, western Africa and western US during months when snowmelt and rainfall runoff are insufficient to meet demands.

Figure 3 maps the snow dependence of basins along two dimensions: the share of irrigation water demand met by snowmelt (colours; Extended Data Fig. 1a) and the magnitude of irrigation water consumption (Supplementary Fig. 5) normalized by basin area (intensity of shading). Snowmelt meets a relatively small share of irrigation demand in basins coloured in green and yellow (<20% and <10%, respectively); irrigation demand in these areas is largely met by rainfall runoff, storage and/or transfers (Fig. 3). The darkest blue basins are those where irrigation water demands are both relatively high (≥1 mm yr^{-1}, when irrigation consumption is normalized by the entire basin area) and substantially (≥30%) met by snowmelt runoff (Fig. 3). These basins are primarily concentrated in high-mountain Asia (the Tibetan Plateau), Central Asia, western Russia, western US and the southern Andes. Together, they encompass ~8% of global population and notable shares of global irrigated crop production: 37% of cotton, 33% of wheat, 23% of maize and 10% of rice (Supplementary Table 1).

Applying the same dimensions of snow dependence (irrigation consumption and the share of that demand met by snowmelt), Fig. 4 shows the monthly snow dependence of specific crops. Globally, rice and cotton in the Northern Hemisphere summer—together with wheat and managed grassland in spring—are particularly snow dependent (the darkest blue cells in Fig. 4). The annual total irrigation surface water consumption varies significantly across crop species, ranging from 0.01 km^3 for cocoa to 200 km^3 for rice.

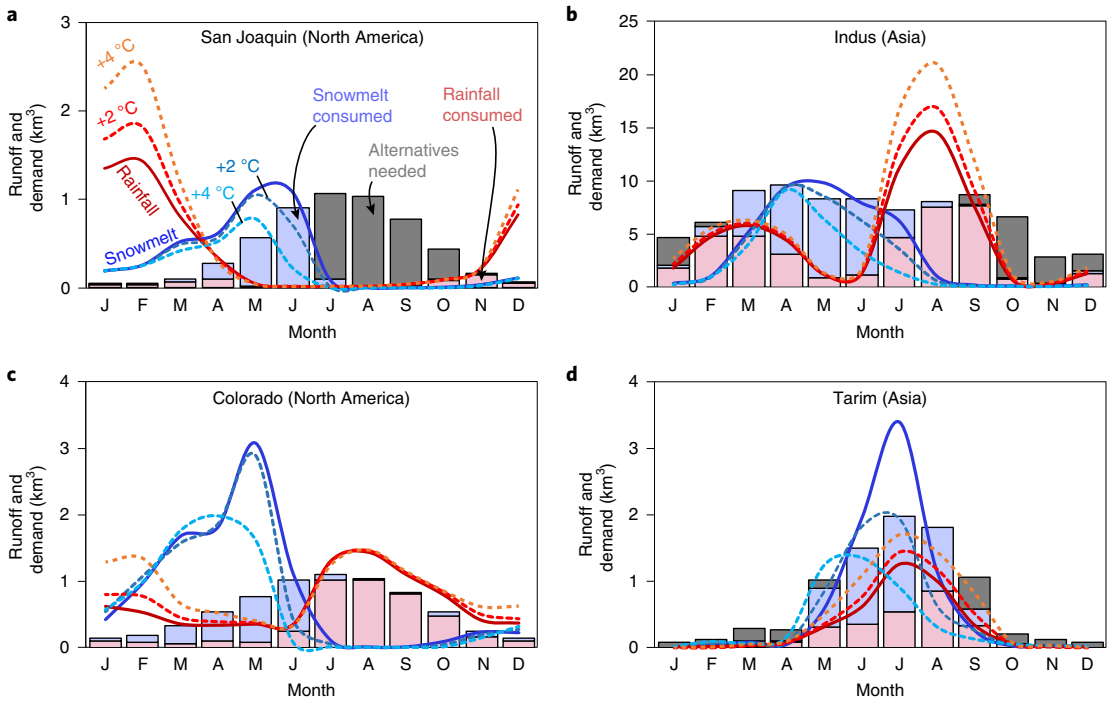

Fig. 2 | Average monthly runoff and surface water demand during recent decades (1985–2015) and runoff under future warming scenarios. a–d, The monthly runoff from rainfall and snowmelt for San Joaquin (North America; **a**), Indus (Asia; **b**), Colorado (North America; **c**) and Tarim (Asia; **d**) are shown, with solid curves showing averages across 1985 to 2015 and dashed curves showing runoff under 2 °C and 4 °C of global warming. For comparison, the stacked bars represent the average monthly surface water consumption by all sectors (1985–2015), where the shaded red, blue and dark grey bars denote the corresponding shares of rainfall, snowmelt and alternative surface water sources (for example, stored in reservoirs and transferred from other basins), respectively.

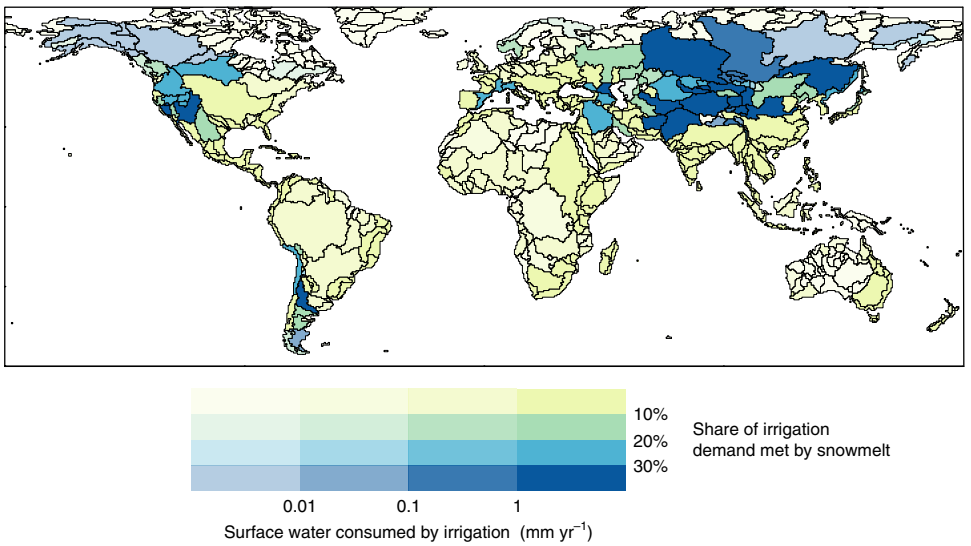

Fig. 3 | Hotspots of snow-dependent irrigated agriculture. Monthly historical data (1985–2015) on surface water supplies and demand are analysed to determine the extent to which basins are reliant on snowmelt runoff to meet irrigation water demand. The colours indicate the average share of irrigation surface water consumption met by snowmelt runoff, whereas the shading indicates the average volume of surface water used for irrigation normalized by basin area. The darkest blue (most snow dependent) basins in high-mountain Asia (the Tibetan Plateau), Central Asia, western Russia, western US and the southern Andes are thus places where both irrigation and the share of irrigation demand met by snowmelt runoff are large. Coastlines are from a modified version[21] of the Simulated Topological Network 30p (ref. [23]).

There are also substantial seasonal variations in irrigation water consumption for each crop (Fig. 4 and Extended Data Fig. 2): wheat consumes the most water in the Northern Hemisphere spring; however, most other crops (for example, date palm, sunflower, soybeans, sorghum, potatoes and pulses) demand the most irrigation water in late summer (July and August) and early autumn

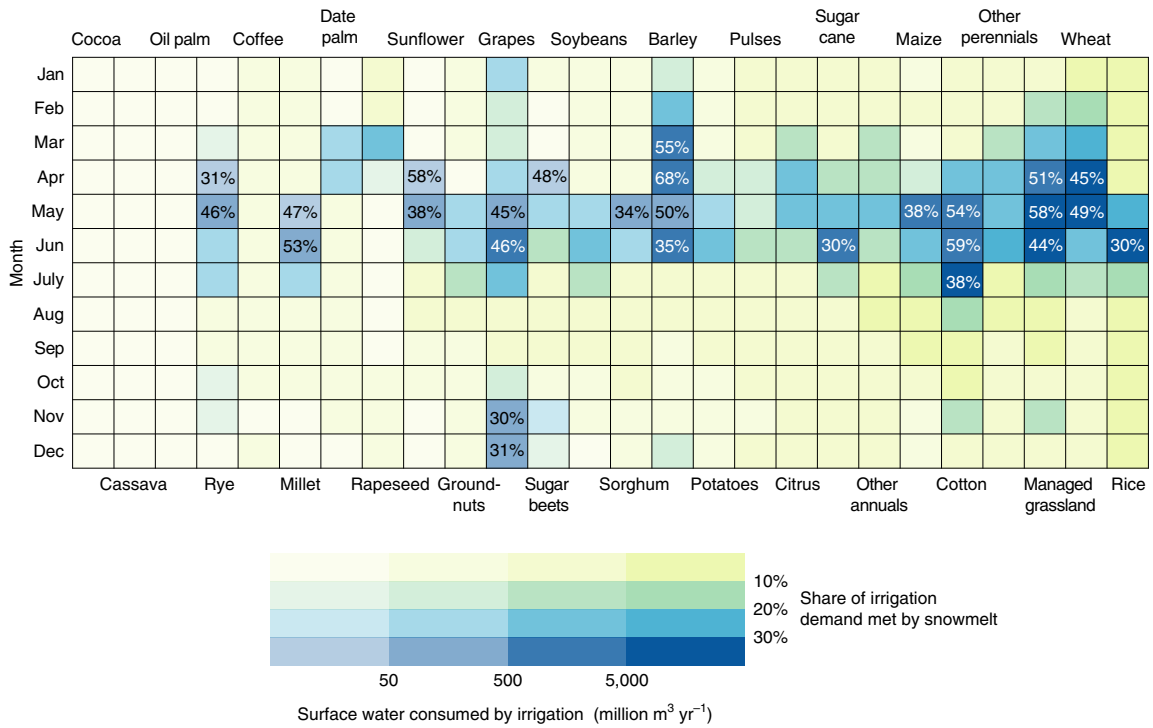

Fig. 4 | Seasonal snowmelt dependence by crop type (1985–2015). Colours indicate the average share of irrigation surface water consumption met by snowmelt runoff, and intensity of shading indicates the average volume of surface water used for irrigation. Large shares of snowmelt consumption (blue colours) occur mostly in spring, and cotton, grassland, wheat and rice are among the most snow-dependent irrigated crops. Crops are ordered by their annual total irrigation surface water consumption, with higher total consumption to the right.

(September), when the share of snowmelt consumed is usually below 10% (Fig. 4). Supplementary Fig. 6 shows regional patterns of monthly, crop-specific snow dependence; crops in Asia are particularly snow dependent.

For basins where agriculture is currently snow dependent (that is, the dark blue basins in Fig. 3), Fig. 5a shows how the shares of current irrigation demand met by snowmelt and alternative sources will change in the future under the 4 °C warming scenario (Extended Data Fig. 3a shows the same changes for the 2 °C warming scenario). All snow-dependent basins see a decrease in the share of irrigation water demand that can be met by snowmelt (Fig. 5a, *x* axis), due to earlier snowmelt availability and/or decreasing total snowmelt runoff under a warming climate. Moreover, in many basins future changes in rainfall do not compensate for the lost snowmelt. If irrigation demands do not change, new alternative sources of water will increasingly be required to meet those demands (Fig. 5a, *y* axis). Basins in the upper-left quadrant of Fig. 5a are likely to experience future challenges and require adaptation efforts; these locations are projected to experience declines in the share of irrigation water met by snowmelt and require increases in alternative water supplies. For instance, in the Po basin of southern Europe, the share of water demand met by snowmelt decreases from 29% to 9% and nearly 40% of irrigation water demands must be met by new alternative sources. Similar changes are observed under the 2 °C warming scenario, though generally to a lesser extent (Extended Data Fig. 3).

To assess risks[28–30] from changing snowmelt by basin, we first define a snowmelt hazard index (SHI) as the product of projected decreases in the share of irrigation demand met by snowmelt runoff (Fig. 5a *x* axis) and expected increases in the share of demand met by alternative water sources (Fig. 5a *y* axis; see also equation (5) in the Methods). Risk further depends on the relative vulnerability[28] of irrigated agriculture in these basins exposed to snowmelt hazards. Vulnerability is influenced by the availability of inter-basin transfers and water storage given geographical, political and economic factors[31,32], and whether additional groundwater extraction is possible and sustainable[33,34]. Reservoir water storage[35] is one indicator of whether basins are equipped to meet such challenges (though we note reservoir storage is not equivalent to the availability of alternative water supplies due to competing reservoir water uses, seasonal fluctuations and possible additional water supplies, including inter-basin transfers). We define a reservoir storage index (RSI) as the ratio of alternative surface water demand to reservoir water storage for every snow-dependent basin (Fig. 5a, dot colours). A lower RSI indicates generally greater flexibility to accommodate increases in alternative water demands via surface water storage. Reservoir water storage is quantified as the minimum of annual excess runoff (runoff of snowmelt or rainfall not utilized in a given month) and current reservoir storage capacity. As shown in Supplementary Table 2, irrigation demands not met by rainfall or snowmelt currently already represent >40% of reservoir water storage in many Asian and North American basins (for example, Amu Darya). Under warming scenarios, demand for alternative water sources in these basins can even increase to >70% of existing reservoir storage (Supplementary Table 2). As basins utilize both groundwater and surface water to meet overall irrigation demand, if surface water availability diminishes, it may be possible to substitute with groundwater; however, some basins (for example, Amu Darya and Syr Darya) almost completely rely on surface water (Supplementary Table 3), indicating heightened vulnerability and adaptation challenges. Additionally, almost all of the basins with a high SHI have relatively low groundwater recharge rates (<100 mm yr^{-1}) (Supplementary Figure 5 in ref. [36]; Supplementary Table 3), so even where groundwater is of suitable quality for irrigation, additional groundwater pumping is likely to be unsustainable. Developing subsurface resources can also be costly and may result in land subsidence, salt intrusions into aquifers and infrastructure damage[37].

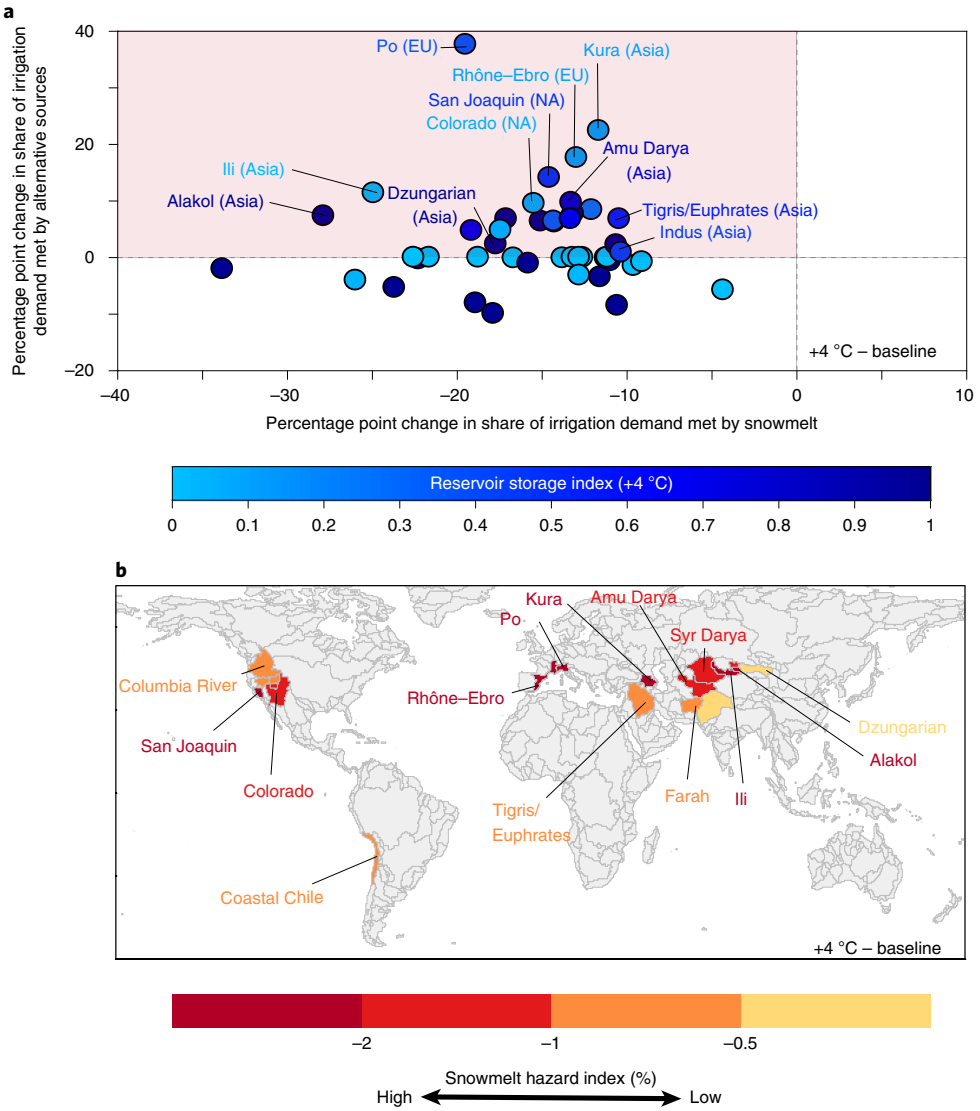

Fig. 5 | Basins at risk from changes in snowmelt under 4 °C warming. a,**b**, The changes in the share of surface water irrigation demand met by snowmelt runoff and alternative water sources for snow-dependent basins are shown in **a**. The *x* axis shows that for all snow-dependent basins, less snowmelt is available during crop-growing seasons to meet irrigation water demand. The *y* axis shows that many basins require an increase in alternative water sources to meet additional water supplies, whereas in some basins the changes in snowmelt are compensated by rainfall runoff. These two factors (*x* and *y* axes in panel **a**) are multiplied together (see Methods) to define a snowmelt hazard index, which is mapped in **b** for all basins in the upper-left quadrant of panel **a**. Dot colours in **a** indicate the reservoir storage index (the ratio of alternative water demand to reservoir water storage). Coastlines are from a modified version[21] of the Simulated Topological Network 30p (ref. [23]). EU, Europe; NA, North America.

Figure 5b maps the snowmelt hazard index for all basins in the top left quadrant of Fig. 5a (red shading) under the 4 °C warming scenario. Basins with a high SHI are primarily located in western US (for example, the San Joaquin basin), southern Europe (the Po and the Rhône–Ebro basins), western China (the Alakol and Ili basins) and Central Asia (the Amu Darya basin) under both warming scenarios (Fig. 5b and Extended Data Fig. 3b).

Our results highlight regions in which irrigated agriculture is currently most dependent on snowmelt runoff, including basin- and crop- specific shares of irrigation water demand now met by snowmelt as well as similarly specific projections of changes in the monthly availability of snowmelt under different levels of future global warming. These findings have large implications for irrigated agriculture and thereby global food security. The most snow-dependent basins currently produce a large fraction of irrigated crops (for example, around 33%, 23% and 10% of irrigated wheat, maize and rice, respectively). We find that irrigated agriculture in many snow-dependent basins is at risk under a changing climate. If at-risk basins are not able to obtain alternative sources of water or substantially improve irrigation efficiency, the location of crops, crop yields and/or the mix of crops could be affected. Such impacts may in turn aggravate the nutrition and food security challenges associated with climate change, which are expected to disproportionately impact the world's poor[38,39]. Our findings can therefore be utilized to prioritize and inform climate adaptation efforts that minimize these impacts by addressing both water supplies (for example, the feasibility of extra groundwater pumping and reservoir development) and water demands (for example, limiting agricultural expansion and increasing crop water productivity).

Several limitations and caveats apply to our study. First, although our model allows for perennial snow, it does not explicitly model glacier dynamics. For example, in Central Asia, accelerated glacier

melting is already well documented, which will lead to consistent and considerable reductions in summer and late spring discharges in a few decades or less[18,20,40], indicating what will most likely be greater risks in these regions than our estimates. Second, our climate change projections utilize multimodel median scaling factors to obtain a central estimate of future change. Future research should more explicitly examine variation between models and how risks are determined by rising temperatures versus comparatively more uncertain precipitation projections[7,18,41]. For simplicity, we have kept water demand static under warming scenarios; however, water consumption is often projected to increase due to rising population, irrigation expansion and higher temperatures[42,43], suggesting that the increasing demands for alternative water sources that we calculate are likely to be conservative. Basin-specific adaptations to existing water management practices will therefore be required and may help offset projected increases in water demand. Here we focus on long-term average runoff and irrigation water demand to characterize agricultural risks under climate change. Future studies should further evaluate potential threats to irrigated agriculture resulting from interannual variations in snowmelt and rainfall runoff. Moreover, although we focus on the agricultural effects of changing snowmelt, other socially, economically and ecologically important water uses will be affected, including energy production, flood control, wildfire risks and reservoir investment/management[44–47].

In addition to efforts to avoid climate change by, for example, developing and advancing renewable energy, energy storage and negative-emission technologies[48–50], efforts to anticipate and adapt to unavoidable climatic changes are critical[46]. Changes in snowpack worldwide are already well documented[13,51,52]. By identifying where, when and which crops are most dependent on snowmelt and most at risk to changes in snowmelt, this work may help guide future research and resources towards those agricultural communities and water management institutions that will most need to adapt to the coming changes.

Online content

Any methods, additional references, Nature Research reporting summaries, source data, extended data, supplementary information, acknowledgements, peer review information; details of author contributions and competing interests; and statements of data and code availability are available at https://doi.org/10.1038/s41558-020-0746-8.

Received: 23 July 2019; Accepted: 6 March 2020;
Published online: 20 April 2020

References

1. Brauman, K. A., Richter, B. D., Postel, S., Malsy, M. & Florke, M. Water depletion: an improved metric for incorporating seasonal and dry-year water scarcity into water risk assessments. *Elem. Sci. Anth.* **4**, 000083 (2016).
2. Oki, T. & Kanae, S. Global hydrological cycles and world water resources. *Science* **313**, 1068–1072 (2006).
3. Portmann, F. T., Siebert, S. & Doll, P. MIRCA2000—Global monthly irrigated and rainfed crop areas around the year 2000: a new high-resolution data set for agricultural and hydrological modeling. *Global Biogeochem. Cycles* **24**, GB1011 (2010).
4. Bruinsma, J. (ed.) *World Agriculture: Towards 2015/2030. An FAO Perspective* (Earthscan, 2003).
5. Alexandratos, N. & Bruinsma, J. *World Agriculture Towards 2030/2050: The 2012 Revision. ESA Working Paper No*. 12-03 (FAO, 2012).
6. Siebert, S. et al. Groundwater use for irrigation—a global inventory. *Hydrol. Earth Syst. Sci.* **14**, 1863–1880 (2010).
7. Jiménez Cisneros, B. E. et al. in *Climate Change 2014: Impacts, Adaptation, and Vulnerability* (eds, Field, C. B. et al) 229–269 (IPCC, Cambridge Univ. Press, 2014).
8. Elliott, J. et al. Constraints and potentials of future irrigation water availability on agricultural production under climate change. *Proc. Natl Acad. Sci. USA* **111**, 3239–3244 (2014).
9. Yu, C. Q. et al. Assessing the impacts of extreme agricultural droughts in China under climate and socioeconomic changes. *Earths Future* **6**, 689–703 (2018).
10. Vano, J. A. et al. Climate change impacts on water management and irrigated agriculture in the Yakima River Basin, Washington, USA. *Clim. Change* **102**, 287–317 (2010).
11. Portmann, F., Siebert, S., Bauer, C. & Döll, P. *Global Dataset of Monthly Growing Areas of 26 Irrigated Crops. Frankfurt Hydrology Paper 06. Institute of Physical Geography* 400 (University of Frankfurt, 2008).
12. Waliser, D. et al. Simulating cold season snowpack: impacts of snow albedo and multi-layer snow physics. *Clim. Change* **109**, 95–117 (2011).
13. Huning, L. S. & AghaKouchak, A. Mountain snowpack response to different levels of warming. *Proc. Natl Acad. Sci. USA* **115**, 10932–10937 (2018).
14. Li, D. Y., Wrzesien, M. L., Durand, M., Adam, J. & Lettenmaier, D. P. How much runoff originates as snow in the western United States, and how will that change in the future? *Geophys. Res. Lett.* **44**, 6163–6172 (2017).
15. Vicuna, S., McPhee, J. & Garreaud, R. D. Agriculture vulnerability to climate change in a snowmelt-driven basin in semiarid chile. *J Water Resour. Plan. Manag.* **138**, 431–441 (2012).
16. Easterling, W. E. et al. in *Climate Change 2007: Impacts, Adaptation and Vulnerability* (Parry, M. L. et al.) 273–313 (IPCC, Cambridge Univ. Press, 2007).
17. Kapnick, S. B. & Delworth, T. L. Controls of global snow under a changed climate. *J. Clim.* **26**, 5537–5562 (2013).
18. Barnett, T. P., Adam, J. C. & Lettenmaier, D. P. Potential impacts of a warming climate on water availability in snow-dominated regions. *Nature* **438**, 303–309 (2005).
19. Adam, J. C., Hamlet, A. F. & Lettenmaier, D. P. Implications of global climate change for snowmelt hydrology in the twenty-first century. *Hydrol. Process.* **23**, 962–972 (2009).
20. Immerzeel, W. W., van Beek, L. P. H. & Bierkens, M. F. P. Climate change will affect the asian water towers. *Science* **328**, 1382–1385 (2010).
21. Mankin, J. S., Viviroli, D., Singh, D., Hoekstra, A. Y. & Diffenbaugh, N. S. The potential for snow to supply human water demand in the present and future. *Environ. Res. Lett.* **10**, 114016 (2015).
22. Abatzoglou, J. T., Dobrowski, S. Z., Parks, S. A. & Hegewisch, K. C. Terraclimate, a high-resolution global dataset of monthly climate and climatic water balance from 1958-2015. *Sci. Data* **5**, 170191 (2018).
23. Vorosmarty, C. J., Green, P., Salisbury, J. & Lammers, R. B. Global water resources: vulnerability from climate change and population growth. *Science* **289**, 284–288 (2000).
24. Siebert, S. & Doll, P. Quantifying blue and green virtual water contents in global crop production as well as potential production losses without irrigation. *J. Hydrol.* **384**, 198–217 (2010).
25. *Food and Agriculture Data* (Food and Agriculture Organization of the United Nations, 2018); http://www.fao.org/faostat/en/#data
26. Hoekstra, A. Y., Mekonnen, M. M., Chapagain, A. K., Mathews, R. E. & Richter, B. D. Global monthly water scarcity: blue water footprints versus blue water availability. *PLoS ONE* **7**, e32688 (2012).
27. Goldewijk, K. K., Beusen, A., Doelman, J. & Stehfest, E. Anthropogenic land use estimates for the Holocene – HYDE 3.2. *Earth Syst. Sci. Data* **9**, 927–953 (2017).
28. IPCC: Summary for Policymakers. In *Climate Change 2014: Impacts, Adaptation, and Vulnerability* (eds Field, C. B. et al.) 1–32 (Cambridge Univ. Press, 2014).
29. Sharma, J. & Ravindranath, N. Applying IPCC 2014 framework for hazard-specific vulnerability assessment under climate change. *Environ. Res. Commun.* **1**, 051004 (2019).
30. Hagenlocher, M. et al. Drought vulnerability and risk assessments: state of the art, persistent gaps, and research agenda. *Environ. Res. Lett.* **14**, 083002 (2019).
31. Ben Fraj, W., Elloumi, M. & Molle, F. The politics of interbasin transfers: socio-environmental impacts and actor strategies in Tunisia. *Nat. Resour. Forum* **43**, 17–30 (2019).
32. Liu, L. et al. Quantifying the potential for reservoirs to secure future surface water yields in the world's largest river basins. *Environ. Res. Lett.* **13**, 044026 (2018).
33. Wada, Y. et al. Global monthly water stress: 2. Water demand and severity of water stress.*Water Resour. Res.* **47**, W07518 (2011).
34. Nelson, K. S. & Burchfield, E. K. Effects of the structure of water rights on agricultural production during drought: a spatiotemporal analysis of California's central valley. *Water Resour. Res.* **53**, 8293–8309 (2017).
35. Lehner, B. C. et al. High-resolution mapping of the world's reservoirs and dams for sustainable river-flow management. *Front. Ecol. Environ.* **9**, 494–502 (2011).
36. Qin, Y. et al. Flexibility and intensity of global water use. *Nat. Sustain.* **2**, 515–523 (2019).
37. Sneed M. & Brandt J. M. S. *Land Subsidence Along the Delta–Mendota Canal in the Northern Part of the San Joaquin Valley, California, 2003–2010* Scientific Investigations Report 2013-5142 (US Geological Survey, 2013); http://pubs.usgs.gov/sir/2013/5142/

38. Godfray, H. C. J. et al. Food security: the challenge of feeding 9 billion people. *Science* **327**, 812–818 (2010).
39. Myers, S. S. et al. Climate change and global food systems: potential impacts on food security and undernutrition. *Annu. Rev. Publ. Health* **38**, 259–277 (2017).
40. Pritchard, H. D. Asia's shrinking glaciers protect large populations from drought stress. *Nature* **569**, 649–654 (2019).
41. Mankin, J. S. & Diffenbaugh, N. S. Influence of temperature and precipitation variability on near-term snow trends. *Clim. Dynam.* **45**, 1099–1116 (2015).
42. Rothausen, S. G. S. A. & Conway, D. Greenhouse-gas emissions from energy use in the water sector. *Nat. Clim. Change* **1**, 210–219 (2011).
43. Schewe, J. et al. Multimodel assessment of water scarcity under climate change. *Proc. Natl Acad. Sci. USA* **111**, 3245–3250 (2014).
44. Bormann, K. J., Brown, R. D., Derksen, C. & Painter, T. H. Estimating snow-cover trends from space. *Nat. Clim. Change* **8**, 923–927 (2018).
45. Knowles, N., Dettinger, M. D. & Cayan, D. R. Trends in snowfall versus rainfall in the Western United States. *J. Clim.* **19**, 4545–4559 (2006).
46. Mote, P. W. Trends in snow water equivalent in the Pacific Northwest and their climatic causes. *Geophys. Res. Lett.* **30**, 12 (2003).
47. Westerling, A. L., Hidalgo, H. G., Cayan, D. R. & Swetnam, T. W. Warming and earlier spring increase western US forest wildfire activity. *Science* **313**, 940–943 (2006).
48. Davis, S. J. et al. Net-zero emissions energy systems. *Science* **360**, eaas9793 (2018).
49. Guan, D. B. et al. Structural decline in China's CO_2 emissions through transitions in industry and energy systems. *Nat. Geosci.* **11**, 551–555 (2018).
50. Davies, D. M. et al. Combined economic and technological evaluation of battery energy storage for grid applications. *Nat. Energy* **4**, 42–50 (2019).
51. Clow, D. W. Changes in the timing of snowmelt and streamflow in colorado: A response to recent warming. *J Clim.* **23**, 2293–2306 (2010).
52. Rasmussen, R. et al. Climate change impacts on the water balance of the colorado headwaters: high-resolution regional climate model simulations. *J. Hydrometeorol.* **15**, 1091–1116 (2014).
53. *The NCAR Command Language v.6. 6.2* (NCAR, 2019); https://doi.org/10.5065/D6WD3XH5

Methods

Historical runoff. Monthly average total runoff for the period of 1985–2015 (1/24°×1/24°) are obtained from a global climate and climatic water balance dataset, TerraClimate, which has demonstrated strong validation with a number of network observations[22]. Using the water balance model, total surface runoff is partitioned into snowmelt runoff and rainfall runoff. The model simulates snowpack accumulation and ablation, as well as the fluxes of water into and out of a single soil layer on monthly time steps. The model allows for perennial snow but does not explicitly model glacier dynamics. Runoff occurs in months with a net surplus of liquid water inputs (rainfall and snowmelt) minus that which is used to saturate the soil column and to satisfy evapotranspiration demands. A total of 5% of monthly liquid water inputs (precipitation plus snowmelt) are converted directly to runoff without being available for soil moisture recharge or evapotranspiration. This parameterization accounts for processes occurring at sub-monthly timescales that contribute directly to runoff. The results of this model compare well with annual streamflow and interannual variability in streamflow across pristine gauges globally[22]. We partitioned the runoff due strictly to snowmelt versus that due to rainfall by prioritizing rainfall water for saturating the soil and satisfying the evapotranspiration demands. On satisfying soil reservoir capacity and evapotranspiration fluxes, excess rainfall goes to runoff. This framework allows snowmelt to have priority for the immediate 5% of runoff not subject to other fluxes; excess snowmelt is then used to satisfy evapotranspiration fluxes and soil moisture recharge not met by rainfall. Surplus snowmelt is then allowed to runoff. More details of the water balance model are described in ref. [22]. Supplementary Fig. 7 shows the validation of the basin-level snow water equivalent from TerraClimate with the Snow Data Assimilation System Data Products at the National Snow and Ice Data Center, which provides the best possible estimates of snow cover and associated properties across central North America[54]. Supplementary Fig. 7 shows that TerraClimate captures both the magnitude and seasonality of snow water equivalent with reasonable accuracy. Grid-level (1/24°×1/24°) ratios of snowmelt runoff to total runoff at both annual average and monthly average levels during the period of 1985–2015 are calculated (Fig. 1, coastlines are from NCL/NCAR: http://www.ncl.ucar.edu/citation.shtml; ref. [53]), which we define as the annual or monthly snowmelt runoff ratio, respectively. This metric directly characterizes the contribution of snowmelt runoff to total runoff during our interested period. Regions with snowmelt runoff ratio ≥50% are considered to be snowmelt dominant.

We aggregate the monthly grid-level snowmelt runoff and rainfall runoff in each year during the period of 1985–2015 to calculate their corresponding average, median and 25th and 75th percentile values for global basins (Fig. 2 and Supplementary Fig. 3). In this study we use the same drainage basin shapefile as used in ref. [21], which is the modified version of the Simulated Topological Network 30p (ref. [23]).

Historical water demand. We calculate monthly crop-specific irrigation water consumption using the Global Crop Water Model (GCWM)[24], which utilizes the Penman–Monteith equation, crop area and growing season information[3], yearly varying climate forcing and daily soil water balances to calculate irrigation water consumption from 1985 to 2015 (1/12°×1/12°). Following ref. [36], we use country-level time series data of areas equipped for irrigation from the Food and Agriculture Organization of the United Nations database[25] to adjust GCWM-simulated irrigation water consumption for each of 26 crop types. As irrigation water consumption includes both surface water and groundwater, we then use the grid-level (1/12°×1/12°) fraction of surface irrigation water[6] to calculate monthly average grid-level crop-specific surface irrigation water consumption during 1985–2015.

We assume that the monthly average water consumption from other sectors (for example, domestic and industry) during this period is the same as that calculated in ref. [26] at a spatial resolution of 1/12°×1/12°. In the absence of better information, we assume the grid-level proportion of surface water consumption to groundwater consumption in these other sectors is the same as that for irrigated agriculture. We then aggregate grid-level surface water consumption in each sector to calculate their corresponding monthly average values for 1985–2015 at the same basin-level as that of snowmelt and rainfall runoff.

Comparison between historical runoff and demand. Comparing basin-average historical runoff and total surface water consumption, we estimate monthly snowmelt runoff consumption, rainfall runoff consumption and demand for alternative water sources in each major river basin. We assume that: (1) once snow melts, snowmelt runoff is used to meet water demands in an equivalent manner as rainfall runoff; (2) all water uses have equal allotment priority; thus, if a basin's monthly total runoff is more than surface water consumption, there is no need for alternative water in that month. Monthly total snowmelt (rainfall) runoff consumption in the basin is then calculated by multiplying the basin total surface water consumption with its corresponding snowmelt runoff ratio (1 minus snowmelt runoff ratio) in that month; however, if the monthly total runoff is less than the monthly total surface water consumption, all snowmelt and rainfall runoff will be consumed, with additional water demand met by alternative surface water sources (for example, water storage and inter-basin transfers). An underlying assumption is that there is enough water to meet historical demand, though alternative surface water sources may have been obtained at high economic costs. Monthly snowmelt runoff, rainfall runoff and alternative water consumption for irrigated agriculture are then estimated based on the monthly fraction of irrigation surface water consumption to total surface water consumption in each basin.

We calculate the basin-level annual average snowmelt consumption ratio for irrigated agriculture (the share of irrigation surface water consumption met by snowmelt runoff). The snowmelt consumption ratio indicates not only the relative importance of snowmelt runoff as a local water source, but also the extent of temporal synchronization between snowmelt runoff availability and irrigation water demand. Each basin's snow dependence is characterized by two dimensions: the snowmelt consumption ratio and basin-average surface water consumption for irrigation. Crop-specific snowmelt consumption ratios are calculated by dividing irrigation snowmelt runoff consumption by total irrigation surface water consumption for each crop.

Warming scenarios. Projections of snowmelt runoff and rainfall runoff are considered for two different levels of change in global climate corresponding with global mean temperature 2 °C and 4 °C above preindustrial conditions. We use a pattern scaling approach to superpose changes in monthly climate variables to TerraClimate historical data for 1985–2015. The pattern scaling approach uses the concept that geographic patterns to climate forcing scale reasonably linearly in response to changes in global mean temperature[55,56]. These patterns can be used to scale changes in global mean annual temperature (G) to local and seasonal changes for a host of climate variables using linear regressions:

$$c(x,y,m) = \frac{\Delta Z(x,y,m)}{\Delta G} \quad (1)$$

where x, y and m represent the longitude, latitude and month for a given climate variable (Z). Scaling factors (c) are developed for monthly climate variables of maximum temperature, minimum temperature, specific humidity, 10 m wind speed, precipitation and surface downward shortwave radiation.

We acquire climate projections from 23 CMIP5 climate models (Supplementary Table 4) for two 30-year periods, a preindustrial period (1850–1879) using historical forcing experiment and an end of the twenty-first century period (2070–2099) using the RCP8.5 forcing experiment. Multimodel median scaling factors (c) for each variable are calculated using the changes in climate between the two 30-year periods.

Future climate scenarios developed by incorporating interpolated pattern scaling with the TerraClimate data for the period of 1985–2015. This approach superposes the changes in climate means and variability with the observed temporal patterns using equation (2) for additive variables.

$$\begin{aligned} Z_f(x,y,m,t) = {} & \tfrac{Z_o(x,y,m,t)-\overline{Z_o(x,y,m)}}{\sigma_o(x,y,m)} \\ & \cdot(\sigma_o(x,y,m)+\Delta\sigma(x,y,m))+ \\ & \left(\overline{Z_o(x,y,m)}+\Delta Z(x,y,m)\right) \end{aligned} \quad (2)$$

$$\Delta Z(x,y,m) = c_z(x,y,m)\times\Delta G \quad (3)$$

$$\Delta\sigma(x,y,m) = c_\sigma(x,y,m)\times\Delta G \quad (4)$$

where t indicates each year from 1985 to 2015; Z is the variable of interest; o and f represent observed and future time series, respectively; the overbar represents 30-year averages; and factors ΔZ and $\Delta\sigma$ represent changes in mean and standard deviation as expressed by multiplying the scaling factors for the mean (c_z) and standard deviation (c_σ), respectively, by the change in G (equations (3) and (4)).

We focus on climate scenarios for global mean temperatures 2 °C and 4 °C above preindustrial levels per policy targets. To account for the fact that we use climate over the period 1985–2015, we multiplied scaling factors (c) by a factor (S) of 1.3 and 3.3 for the 2 °C and 4 °C scenarios given that both observations and climate model experiments show that global mean annual temperature for the 1985–2015 period was approximately 0.7 °C greater than preindustrial levels[57,58]. Although we utilize multimodel median scaling factors to provide a central estimate of future changes, pattern scaling does allow evaluation of model spread in scaling factors; for example, the multimodel median land warming (averaged across all months) is 1.22 °C per °C of global mean temperature, with an interquartile range of 0.1 °C per °C.

The pattern scaling approach is computationally inexpensive and hence can be downscaled to a high-spatial resolution. Using this approach, scenarios can be developed without having to be explicitly tied to emission scenarios and time periods. Rather, the approach is highly flexible in that it allows for interoperability between uncertainty inherent in models, emission scenarios and time periods, and can be used to explicitly develop climate scenarios targeted to policy-relevant goals such as 2 °C and 4 °C above preindustrial levels[59].

Water balance models running with 2 °C and 4 °C scenarios use monthly data from TerraClimate during 1985–2015 superposed with pattern scaling. We modify

reference evapotranspiration using a correction factor that reduces atmospheric demand with increased CO_2 to account for potential changes in landscape evapotranspiration due to rising levels of CO_2 (ref. [60]). We approximate increases in CO_2 of 150 ppm and 385 ppm from 1985–2015 baselines, corresponding with global mean temperatures of 2 °C and 4 °C above preindustrial, respectively[60].

Following the same method as used for the baseline climate, we further estimate the monthly mean irrigation surface water consumption originating from snowmelt runoff, rainfall runoff and alternative sources under both the 2 °C and 4 °C warming scenarios. By comparing the percentage point changes in the share of irrigation surface water demand met by snowmelt runoff (Δ snowmelt consumption ratio) and alternative sources (Δ alternative water demand ratio) between warming scenarios and the baseline for basins with relatively high snow dependence (that is, basins in which ≥20% of runoff is snowmelt and basin-average irrigation surface water consumption ≥0.1 mm yr^{-1}), we identify basins that are exposed to changing snowmelt hazards. We calculate a SHI (equation (5)) for basins with decreases in their snowmelt consumption ratio (Δ snowmelt consumption ratio < 0) and increases in their alternative water demand ratio (Δ alternative water demand ratio > 0).

$$\mathrm{SHI} = \Delta\ \text{snowmelt consumption ratio} \times \Delta\ \text{alternative water demand ratio} \quad (5)$$

Decreasing snowmelt consumption ratio indicates decreases in snowmelt runoff during crop-growing seasons due to earlier melting and/or decreasing magnitude (Fig. 5a, *x* axis). These basins may or may not suffer from such changes; in some basins, rainfall runoff can compensate for the decreasing snowmelt; however, in other basins, new alternative sources of water will increasingly be required to meet those demands (Fig. 5a, *y* axis). Alternative sources could include further exhausting existing intra-basin storage, expanding intra-basin storage, increasing inter-basin transfers, desalination, and increasing groundwater extraction beyond current levels.

We additionally evaluate the potential availability of reservoir storage and groundwater, which affect the vulnerability of each basin. We develop a Reservoir Storage Index (RSI; Supplementary Table 2) by comparing alternative water demands to reservoir water storage, where water storage is defined as the minimum of annual excess runoff (runoff of snowmelt or rainfall not utilized in a given month) and reservoir storage capacity from the Global Reservoir and Dam Database v.1.3 (ref. [35]). Note in Fig. 5a, RSI is treated as ≫1 for basins without recorded reservoir capacity while requiring alternative demand. We also evaluate the feasibility of using groundwater resources to meet future water demands by examining the current percentage of irrigation demand supplied by groundwater and recharge rates (Supplementary Table 3). The snowmelt hazard index is mapped in Fig. 5b to highlight regions most at risk and in need of climate adaptation strategies.

Data availability

The numerical results plotted in Fig. 1 is available from figshare: https://doi.org/10.6084/m9.figshare.12016254.v1; numerical results for Figs. 2–5 and the Extended Figures are provided with this paper. TerraClimate data is available from: http://www.climatologylab.org/terraclimate.html and GCWM outputs are available from: https://www.uni-frankfurt.de/45217988/Global_Crop_Water_Model__GCWM. All other data that support the findings of this study are available in the main text or the Supplementary Information.

Code availability

Computer code or algorithm used to generate results that are reported in the paper and central to the main claims are available from the corresponding authors on reasonable request.

References

54. *Snow Data Assimilation System (SNODAS) Data Products at NSIDC, Version 1* (NSIDC, accessed December 2018); https://doi.org/10.7265/N5TB14TC
55. Mitchell, T. D. Pattern scaling—an examination of the accuracy of the technique for describing future climates. *Clim. Change* **60**, 217–242 (2003).
56. Huntingford, C. & Cox, P. M. An analogue model to derive additional climate change scenarios from existing GCM simulations. *Clim. Dynam.* **16**, 575–586 (2000).
57. Kirtman, B. et al. in *Climate Change 2013: The Physical Science Basis* (eds Stocker, T. F. et al.) Ch. 11 (IPCC, Cambridge Univ. Press, 2013).
58. Hawkins, E. et al. Estimating changes in global temperature since the preindustrial period. *Bull. Am. Meteorol. Soc.* **98**, 1841–1856 (2017).
59. James, R., Washington, R., Schleussner, C. F., Rogelj, J. & Conway, D. Characterizing half-a-degree difference: a review of methods for identifying regional climate responses to global warming targets. *WIRES Clim. Change* **8**, e457 (2017).
60. Kruijt, B., Witte, J. P. M., Jacobs, C. M. J. & Kroon, T. Effects of rising atmospheric CO_2 on evapotranspiration and soil moisture: a practical approach for the Netherlands. *J. Hydrol.* **349**, 257–267 (2008).

Acknowledgements

This work was supported by the Foundation for Food and Agriculture Research through a New Innovator Award to N.D.M., by the US National Science Foundation INFEWS grant EAR 1639318 to S.J.D., and by the German Federal Ministry of Education and Research (BMBF; grant no. 02WGR1457F) through its Global Resource Water (GRoW) funding initiative to S.S.

Author contributions

N.D.M., S.J.D. and Y.Q. designed the study. Y.Q. performed the analyses, with additional support from J.T.A., S.S., L.S.H., A.A., J.S.M. on datasets and S.S., J.T.A., J.S.M., C.H. and D.T. on analytical approaches. Y.Q., N.D.M., S.J.D. and J.T.A. led the writing with input from all co-authors.

Competing interests

The authors declare no competing interests.

Additional information

Extended data is available for this paper at https://doi.org/10.1038/s41558-020-0746-8.

Supplementary information is available for this paper at https://doi.org/10.1038/s41558-020-0746-8.

Correspondence and requests for materials should be addressed to Y.Q. or N.D.M.

Peer review information *Nature Climate Change* thanks Tobias Siegfried and Julie Vano for their contribution to the peer review of this work.

Reprints and permissions information is available at www.nature.com/reprints.

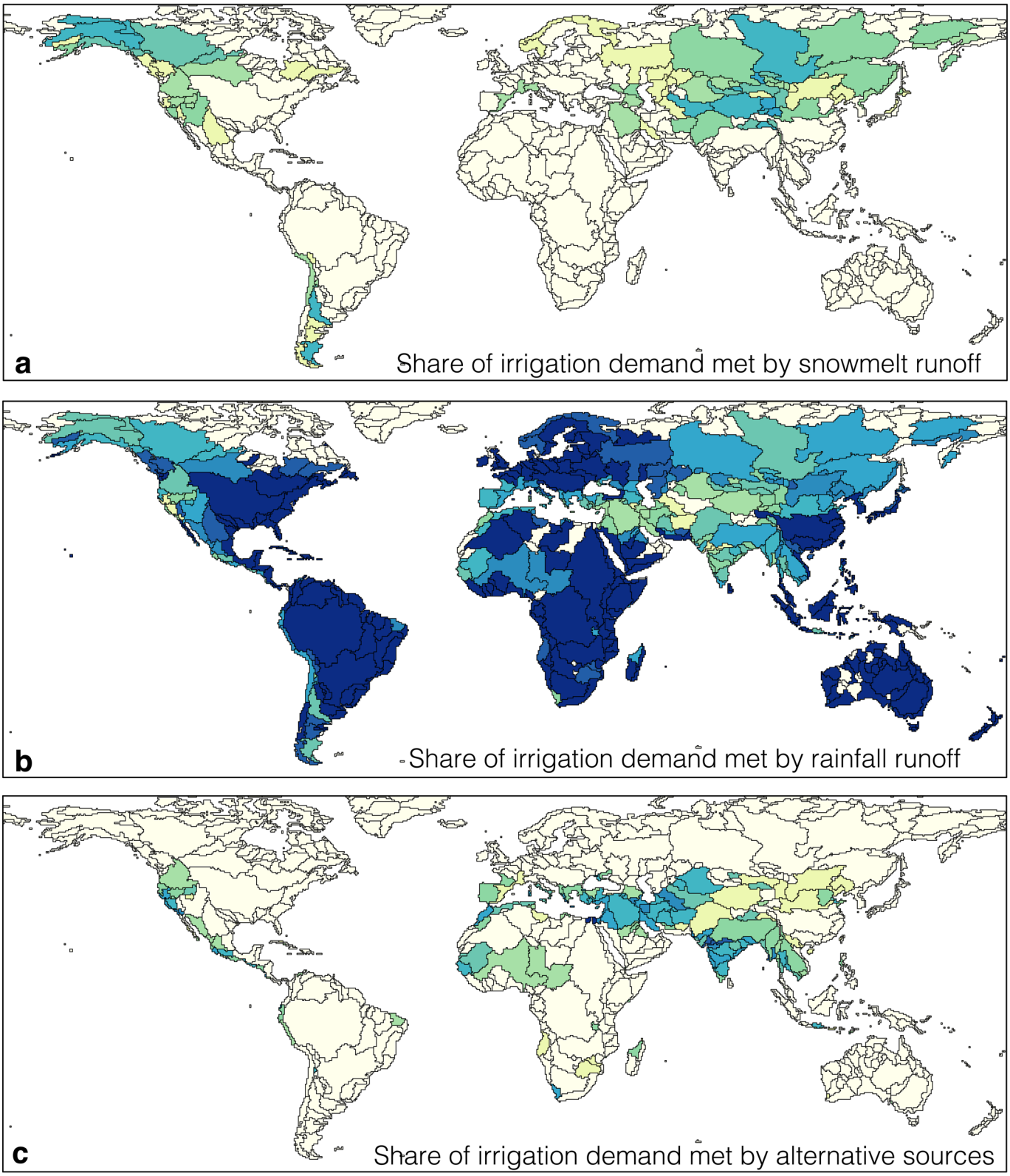

Extended Data Fig. 1 | Share of annual average irrigation surface water consumption 1985–2015 met by different sources. Share of annual average irrigation surface water consumption 1985–2015 met by (**a**) snowmelt runoff, (**b**) rainfall runoff, and (**c**) alternative sources (for example, water stored in reservoirs and inter-basin transfers). Shares from all three sources are zero for basins without irrigation surface water consumption.

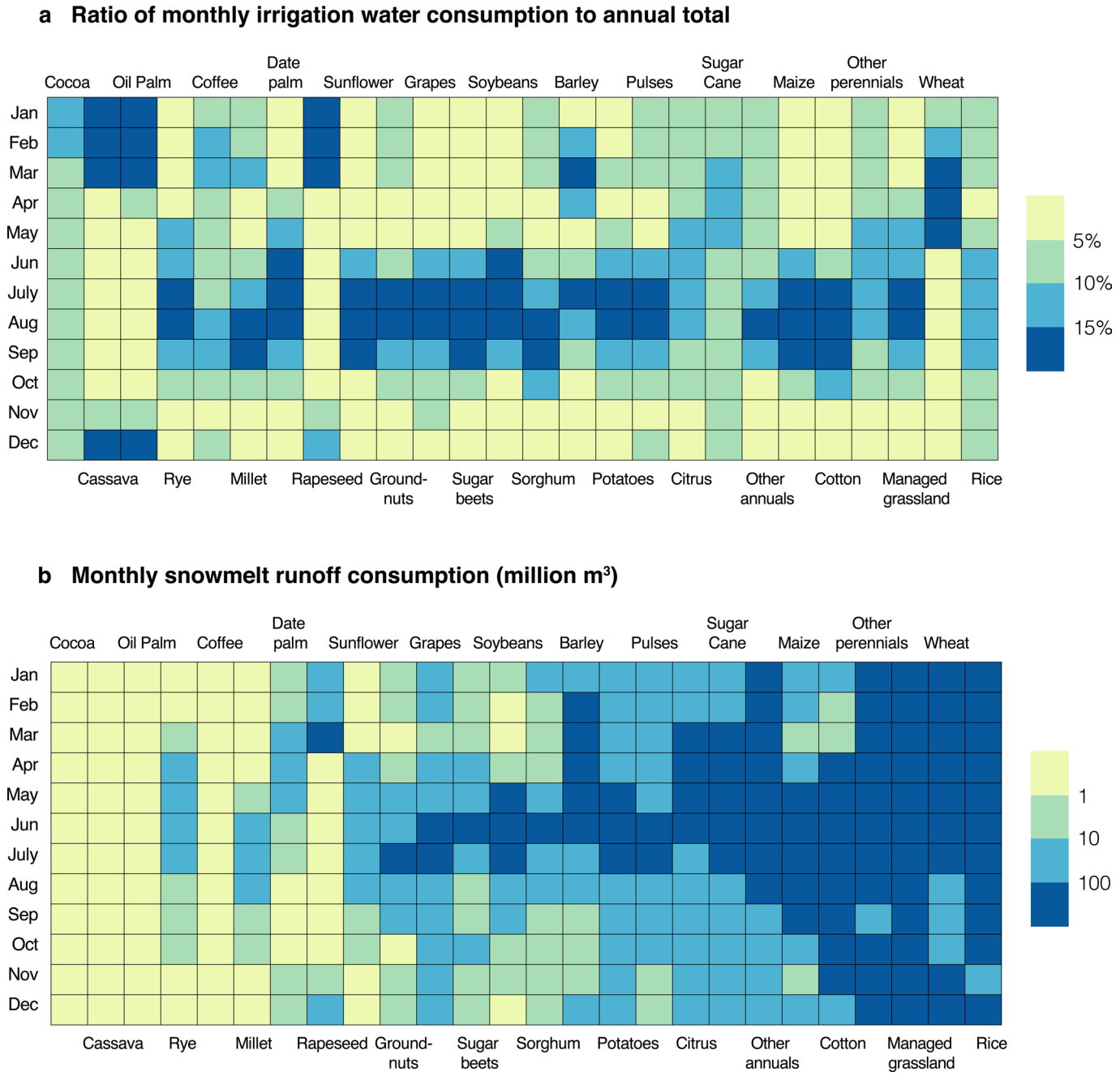

Extended Data Fig. 2 | Monthly and crop-specific irrigation share and snow consumption. Crop-specific (**a**) monthly ratio of irrigation surface water consumption to corresponding annual total, and (**b**) monthly snowmelt runoff consumption for the period of 1985–2015. Crops are ordered by their annual total irrigation surface water consumption, with higher total consumption to the right.

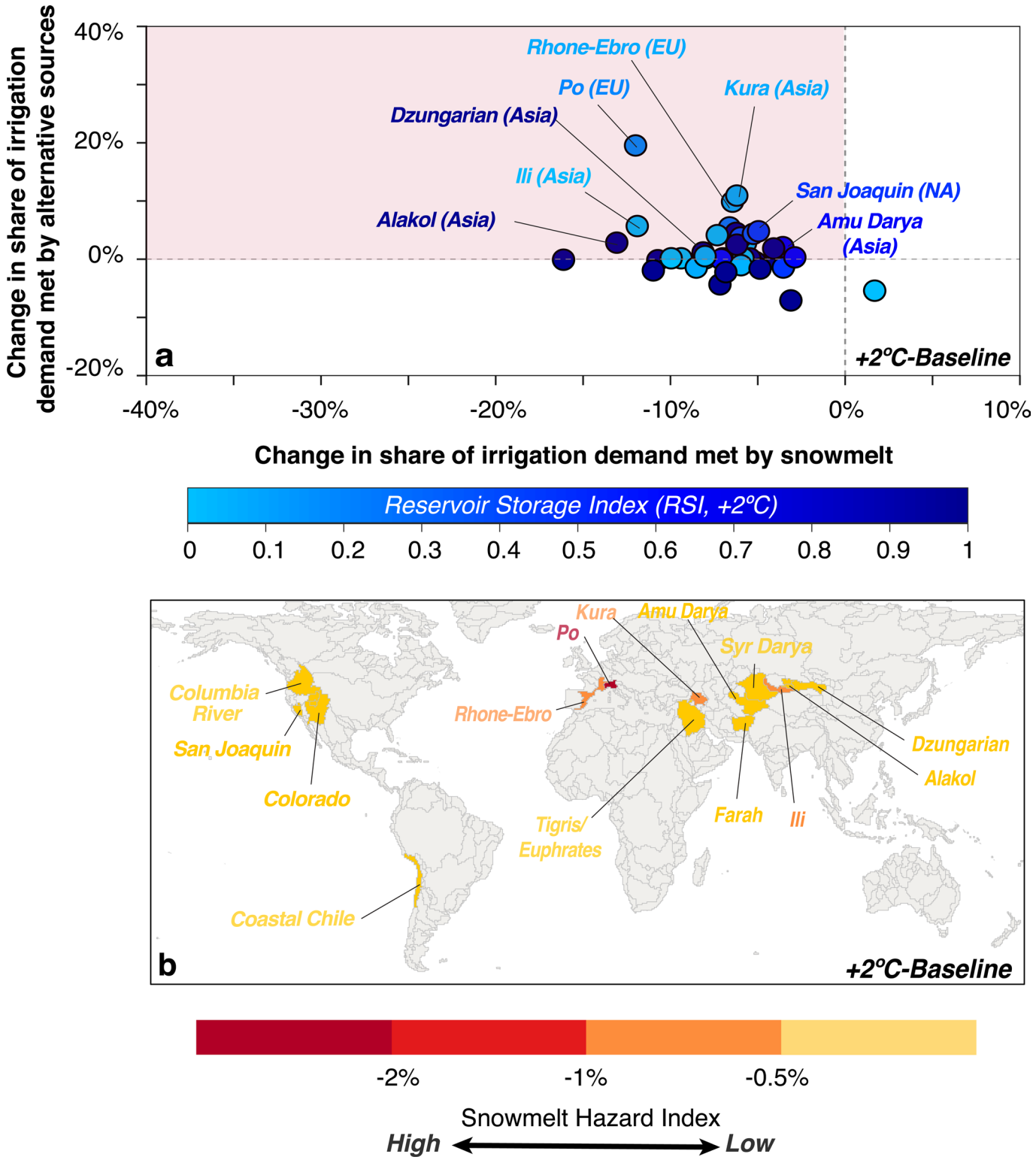

Extended Data Fig. 3 | Changes in irrigation surface water from snowmelt and alternative sources under 2 °C warming for snow-dependent basins. Details of this figure are identical to Fig. 5, except displayed for 2 °C warming.